Origin of Bonding Interactions in $Cu^+(H_2)_n$ Clusters: An Experimental and Theoretical Investigation

Paul R. Kemper,† Patrick Weis,† Michael T. Bowers,*,† and Philippe Maître‡

Contribution from the Department of Chemistry, The University of California at Santa Barbara, Santa Barbara, California 93106-9510, and Laboratoire de Chimie Théorique, Université de Paris-Sud, Centre d'Orsay, 91405 Orsay Cedex

Received June 29, 1998. Revised Manuscript Received October 29, 1998

Abstract: Binding energies and entropies have been measured for the attachment of up to six H_2 ligands to ground-state Cu^+ ions (^1S, $Ar3d^{10}$), to electronically excited Cu^{+}* ions ($^{1,3}D$, $Ar4s^13d^9$), and to hydrated $H_2O{\cdot}Cu^+$ ions. The ground-state Cu^+ ion added four H_2 ligands in the first solvation shell with bond dissociation energies (BDEs) of 15.4, 16.7, 8.8, and 5.1 kcal/mol. The fifth and sixth ligands begin a new solvation sphere and were very weakly bound. The BDEs for addition of H_2 to electronically excited Cu^{+}* were also small (4.2, 2.5, and 1.4 kcal/mol for the first three ligands). The difference between ground- and excited-state association energies is almost entirely due to the repulsive nature of the 4s electron. Hydration of the Cu^+ ion significantly increased the BDE of the first H_2 ligand (to 19.6 kcal/mol) but greatly reduced that of the second (to 3.8 kcal/mol). Theoretical calculations with large basis sets at the DFT-B3LYP and MP2 levels were done on all species both to determine geometries and vibration frequencies and to examine the origin of the bonding and its variation with Cu^+ coordination. The calculations show that covalent interactions are important in these Cu^+ clusters and that the observed changes in BDE as different ligands are added are due to electronic rather than steric effects. These sources of bonding are discussed, and comparisons are made to the $Co^+(H_2)_n$ and $Ni^+(H_2)_n$ systems. It is also shown that the M^+-ligand interactions are similar for H_2 and CO ligands. Special attention is paid to the origin of the highly symmetric D_{3h} planar structure found in $Ni^+(H_2)_3$, $Cu^+(H_2)_3$, and $Cu^+(CO)_3$.

Introduction

In the past 10 years, our understanding of the bonding present in gas-phase transition metal ion clusters has evolved from a simple electrostatic view to an appreciation of the complex factors actually present. The experiments of Kubas et al.[1] first showed that H_2 could be attached as an uninserted species to an oxidized transition metal center. Since then, systematic experiments have examined the role of the metal ion in a large number of gas-phase $M^+{\cdot}X_n$ clusters. Relatively simple systems with $X = H_2$,[2−9] CO,[10,11] and the rare gases[12] have been examined, as well as saturated and unsaturated hydrocarbons and a variety of other species.[13] The strong influence of the nature of the metal ion on both bonding energies and structures in these clusters clearly shows the presence of covalent forces in the bonding. This is reinforced by noting the large difference in M^+-H_2 bond energies between the truly inert alkali ions and the transition metals.[14] Our efforts, in conjunction with many theoretical investigations [13,15−18] have identified a number of these covalent forces. First is the electron donation from the H_2 σ orbital to the metal which stabilizes the ion charge.[13,16,18] Most of this donation is to the metal 4s orbital with a minor amount to the 3d orbital of the proper symmetry. Second, in

* Address correspondence to this author.
† The University of California at Santa Barbara.
‡ Université de Paris-Sud.

(1) Kubas, G. J.; Ryan, R. R.; Swanson, B. I.; Vergamini, P. J.; Wasserman, H. J. *J. Am. Chem. Soc.* **1984**, *106*, 451.
(2) Bushnell, J. E.; Kemper, P. R.; Maître P.; Bowers, M. T. *J. Am. Chem. Soc.* **1994**, *116*, 9710.
(3) Bushnell, J. E.; Kemper, P. R.; Maître P.; Bowers, M. T. *J. Chem. Phys.* **1997**, *106*, 10153.
(4) Bushnell, J. E.; Kemper, P. R.; Bowers, M. T. *J. Phys. Chem.* **1993**, *97*, 11628.
(5) Kemper, P. R.; Weis, P.; Bowers, M. T. *Int. J. Mass Spectrom. Ion Phys.* **1997**, *160* 17.
(6) Kemper, P. R.; Weis, P.; Bowers, M. T. *J. Phys. Chem. A* **1997**,*101*, 2809.
(7) Bushnell, J. E.; Kemper, P. R.; Bowers, M. T. *J. Phys. Chem.* **1995**, *99*, 15602.
(8) (a) Bushnell, J. E.; Kemper, P. R.; von Helden, G.; Bowers, M. T. *J. Phys. Chem.* **1993**, *97*, 52. (b) Kemper, P. R.; Bushnell, J.; van Koppen, P. A. M.; Bowers, M. T. *J. Phys. Chem.* **1993**, *97*, 1810.
(9) Kemper, P. R.; Weis, P.; Bowers, M. T. *Chem. Phys. Lett.* **1998**, *293*, 503.
(10) (a) Sievers, M. R.; Armentrout, P. B. *J. Phys. Chem.* **1995**, *99*, 8135. (b) Khan, F. A.; Clemmer, D. E.; Schultz, R. H.; Armentrout, P. B. *J. Phys. Chem.* **1993**, *97*, 7978. (c) Schultz, R. H.; Crellin, K. C.; Armentrout, P. B. *J. Am. Chem. Soc.* **1991**, *113*, 8590. (d) Goebel, S.; Haynes, C. L.; Khan, P. A.; Armentrout, P. B. *J. Am. Chem. Soc.* **1995**, *117*, 6994. (e) Khan, F. A.; Steele, D. L.; Armentrout, P. B. *J. Phys. Chem.* **1995**, *99*, 7819.
(11) Meyer, F.; Chen, Y.-M.; Armentrout, P. B. *J. Am. Chem. Soc.* **1995**, *117*, 4071.
(12) Kemper, P. R.; Hsu, M.-T.; Bowers, M. T. *J. Phys. Chem.* **1991**, *95*, 10600.
(13) For a general discussion, see: Bauschlicher, C. W.; Partridge, H.; Langhoff, S. R. In *Organometallic Ion Chemistry*; Freiser, B. S., Ed.; Kluwer Academic: Dordrecht, The Netherlands, 1996.
(14) Bushnell, J. E.; Kemper, P. R.; Bowers, M. T. *J. Phys. Chem.* **1994**, *98*, 2044.
(15) (a) Bauschlicher, C. W.; Partridge, H.; Langhoff, S. R *J. Chem. Phys.* **1989**, *91*, 4733. (b) Partridge, H.; Bauschlicher, C. W.; Langhoff, S. R *J. Phys. Chem.* **1992**, *96*, 5350. (c) Bauschlicher, C. W.; Partridge, H.; Langhoff, S. R *Chem. Phys. Lett.* **1990**, *165*, 272.
(16) Maître, P.; Bauschlicher, C. W. *J. Phys. Chem.* **1995**, *99*, 6836.
(17) (a) Maître, P.; Bauschlicher, C. W. *J. Phys. Chem.* **1995**, *99*, 3444. (b) Perry, J. K.; Ohanessian, G.; Goddard, W. A. *J. Phys. Chem.* **1993**, *97*, 5238. (c) Bauschlicher, C. W.; Partridge, H.; Langhoff, S. R *J. Phys. Chem.* **1992**, *96*, 2475.
(18) Maître, P.; Bauschlicher, C. W. *J. Phys. Chem.* **1993**, *97*, 11912.

10.1021/ja9822658 CCC: $15.00
Published on Web 12/10/1998

the late metal ions with filled 3d orbitals, donation to the H_2 σ^* orbital occurs from the metal dπ orbitals.[13,17,18] There are two benefits from this back-donation: greater σ donation occurs because electron density is returned to the H_2 ligands, and 3d−3d exchange stabilization on the metal increases. Third, in ions with half-filled 3dσ orbitals, a hybridization between the $3d_{z^2}$ and the 4s orbital occurs which reduces on-axis Pauli repulsion.[13,15,17,18] Fourth, the 4p orbitals, while significantly higher in energy, may still play a significant structural role.[13,17] Finally, the noncovalent electrostatic interactions (charge-induced dipole and charge quadrupole) are present but usually comprise a small fraction of the total bond strength.[13,14,15] The relative importance of these five factors depends strongly on the valence configuration of the metal ion. The 4s orbital is especially critical, and its occupation is always severely destabilizing.[6,12,13]

Among the late transition metals we have used both theory and experiment to examine $M^+(H_2)_n$ clusters with M = Fe, Co, and Ni,[7,8,9] while Bauschlicher and Maître[17a] and Perry and Goddard[17b] have done very high level calculations on the $Co^+(H_2)_n$ system. These metal ions all have relatively strong bond dissociation energies (BDEs) and similar structures for the first and second clusters. Very different structures are found for larger numbers of ligands, however. In the third cluster, both Fe and Co assume a "T" shape[7,17] while Ni has a planar D_{3h} geometry.[9] In the fifth cluster, Fe and Co both form distorted square pyramids while $Ni^+(H_2)_5$ is a trigonal bipyramid. Both Fe and Co have six H_2 ligands in their nearly octahedral first solvation spheres while Ni has only five.

The Cu^+ ion differs from other late metals in having a filled 3d valence shell in its ground state.[19] It is of interest to see the effect of this filled 3d shell on the M^+-H_2 interaction, especially the importance of electron holes in the 3dσ orbital (present in Ni^+ and Co^+, absent in Cu^+). In addition, the $Cu^+(H_2)_n$ clusters can be compared with the analogous $Cu^+(CO)_n$ ions[11] to establish the extent to which the bonding forces present in $Cu^+(H_2)_n$ apply to other systems. Toward these ends, we present here a combined experimental and theoretical study of $Cu^+(H_2)_n$.

In addition to the clusters with a ground-state Cu^+ core (^{1}S, $3d^{10}$), we also describe the bonding of metastable excited ($4s^13d^9$) Cu^{+*} ions. Our aim here is a comparison with other 4s-containing metals, especially Zn^+, which has been examined previously.[6] Finally, bond strengths of H_2 ligands in $H_2O\cdot Cu^+(H_2)_{1,2}$ ions were also measured to determine the differential effects on subsequent bonding caused by an H_2 or H_2O first ligand.

Experimental Section

Experimental details have been given previously.[2,5,20] Briefly, the Cu^+ ions are formed in a glow discharge ion source using an Ar bath gas. The isotope of interest (either $^{63}Cu^+$ or $^{65}Cu^+$) is mass selected in the first quadrupole and injected into a drift/reaction cell filled with typically 10 Torr of H_2. The ions' excess kinetic energy is rapidly thermalized by collisions. An equilibrium between the various $Cu^+(H_2)_n$ cluster products ($n = 0-6$) is quickly established as the ions are moved through the 4 cm long cell with a small electric field. The field is small enough that no measurable perturbation of the thermodynamic temperature occurs. The ions then exit the cell and are mass analyzed in a second quadrupole. The resulting mass peaks are recorded and integrated and together with the pressure of H_2 (p_{H_2}) are used to calculate the equilibrium constant (K_p):

$$K_p^\circ = \frac{Cu^+(H_2)_n(760)}{Cu^+(H_2)_{n-1}p_{H_2}} \qquad (1)$$

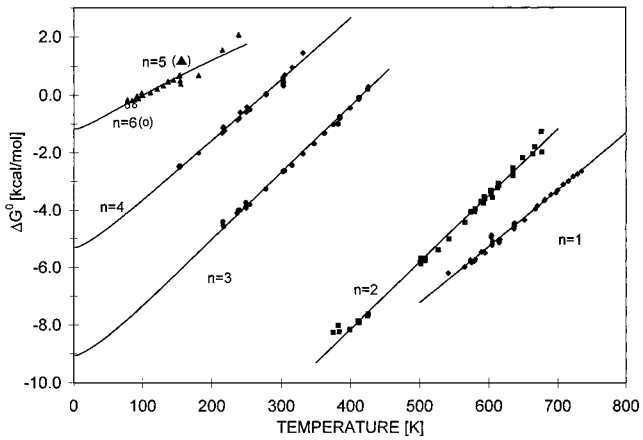

Figure 1. Plot of experimental ΔG_T° vs temperature for the association reaction $Cu^+(H_2)_{n-1} + H_2Cu^+(H_2)_n$. Data for ground-state Cu^+ ($3d^{10}$) reactants are shown. The $n = 6$ data are the open circles below 100 K. The solid lines are statistical mechanical fits to the data which yield values of ΔH_0° at $T = 0$ K (see text).

The standard free energy is then found using eq 2.

$$\Delta G_T^\circ = -RT \ln K_p^\circ \qquad (2)$$

Measurements are taken as a function of temperature from 77 to 780 K. The resulting plots of ΔG_T° vs T are linear over the experimental temperature range with ΔH_T° and ΔS_T° as the intercept and slope, respectively. The linearity of these plots shows that ΔH_T° and ΔS_T° are only very weak functions of temperature over the experimental temperature range. The experimentally determined ΔH_T° and ΔS_T° values for a particular association reaction are used, together with the theoretically determined structure and vibrational frequencies, to determine the heat of reaction at 0 K. The BDE is $-\Delta H_0^\circ$.

Electronic state chromatography experiments[21] showed that both ground-state (^{1}S, $3d^{10}$) and electronically excited Cu^{+*} (^{1,3}D, $4s^13d^9$) were present in our experiment. The excited state was extraordinarily resistant to collisional deactivation by H_2. The use of very high ion injection energies (800 eV) did minimize the amount of excited Cu^{+*} but could not eliminate it. Ordinarily, this would be a minor annoyance; however, in this case, the persistence of the Cu^{+*} ion allowed the association reactions of both ground-state and electronically excited copper ions to be examined separately. This was possible, despite the identical product masses, because of the large difference in BDEs in the two groups. At high temperatures, no measurable excited-state clustering occurred and the more strongly bound ground-state $Cu^+(H_2)_n$ could be examined. At low temperatures the equilibria between the weakly bound $Cu^{+*}(H_2)_{1,2,3}$ ions with H_2 could be measured since all of the ground-state Cu^+ had reacted to form the $Cu^+(H_2)_4$ terminal ion. Plots of vs T for the ground- and excited-state association reactions are shown in Figures1 and 2; data for the association of $H_2O\cdot Cu^+(H_2)_{n-1}$ with H_2 are shown in Figure 3.

Theory

The product ions discussed here were all examined theoretically both to determine the molecular parameters needed to analyze the experimental data and to identify factors important in the bonding. Calculations were carried out at the DFT level using the B3LYP functional[22,23] on both ground state and

(19) Moore, C. E. *Atomic Energy Levels*; U.S. National Bureau of Standards: Washington, DC, 1952; Vol. Circ. 467.
(20) Kemper, P. R.; M. T. Bowers, *J. Am. Soc. Mass Spectrosc.* **1990**, *1*, 197.
(21) (a) Kemper, P. R.; Bowers, M. T. *J. Phys. Chem.* **1991**, *95*, 5134. (b) Bowers, M. T.; Kemper, P. R.; von Helden, G.; van Koppen, P. A. M. *Science* **1993**, *260*, 1446.
(22) Stevens, P. J.; Devlin, F. J.; Chablowski, C. F.; Frisch, M. J. *J. Phys. Chem.* **1994**, *98*, 11623.
(23) Becke, A. D. *J. Chem. Phys.* **1993**, *98*, 5648.

Table 1. Data Summary for $Cu^+(H_2)_n$ Clusters

	experiment				theory		
ion	BDE (D_0)[a]	$-\Delta H_T^\circ$ [a]	$-\Delta S_T^\circ$ [b]	T [c]	symmetry	D_e[a]	D_0[a]
$Cu^+(H_2)$	15.4 ± 1.0[d]	17.1 ± 0.8	19.7 ± 2	650 ± 100	C_{2v}	18.6,[e] 18.1[f]	16.6,[e] 16.2[f]
$Cu^+(H_2)_2$	16.7 ± 1.0[d]	17.6 ± 0.8	23.6 ± 2	525 ± 150	D_{2d}	20.5,[e] 17.9[f]	17.2,[e] 14.5[f]
					D_{2h}	20.3[e]	17.0[e]
$Cu^+(H_2)_3$	8.8 ± 0.5[d]	9.5 ± 0.4	22.7 ± 2	330 ± 110	D_{3h} planar[i]	11.1,[e] 12.0[f]	8.0,[e] 8.6[f]
					D_{3h} vertical[i]	7.4[e]	T. S.
$Cu^+(H_2)_4$	5.1 ± 0.6[d]	5.7 ± 0.5	20.6 ± 2	250 ± 100	D_{2d} (tetra.)	5.5,[e] 5.8[f]	4.6,[e] 4.9[f]
$Cu^+(H_2)_5$	1.0 ± 0.2[g]	1.2 ± 0.2	12.5 ± 2	125 ± 50	C_s planar[i]	−0.1,[e] −2.9[f]	
					C_s vertical[i]	−3.3,[e] −5.3[f]	
$Cu^+(H_2)_6$	1.0 ± 0.3[h]	−	−	77			
$Cu^{+*}(H_2)$	4.2 ± 0.3[d]	4.7 ± 0.3	14.6 ± 2	200 ± 60	C_{2v}	6.5[e]	5.5[e]
$Cu^{+*}(H_2)_2$	2.5 ± 0.4[d]	2.9 ± 0.3	10.8 ± 2	150 ± 70	C_2	5.3[e]	4.1[e]
$Cu^{+*}(H_2)_3$	1.4 ± 0.3[g]	1.9 ± 0.2	10.9 ± 2	100 ± 25	C_1 ($\sim C_3$)	2.9[e]	1.5[e]

[a] In kcal/mol. BDE $\equiv -\Delta H_0^\circ$. [b] In cal/(mol·K). [c] In Kelvin, ± refers to temperature range, not uncertainty. [d] Fitting with theoretical frequencies and geometries. [e] DFT geometries. [f] MP2 geometries. [g] Fitting with ΔC_p correction; error small at low temperature. [h] Fit by correspondence with fifth cluster; not enough data for ΔS and ΔH measurement. [i] Orientation of equatorial H_2 ligands with respect to the equatorial (xy) plane. The more stable planar structure has all six H atoms in the xy plane.

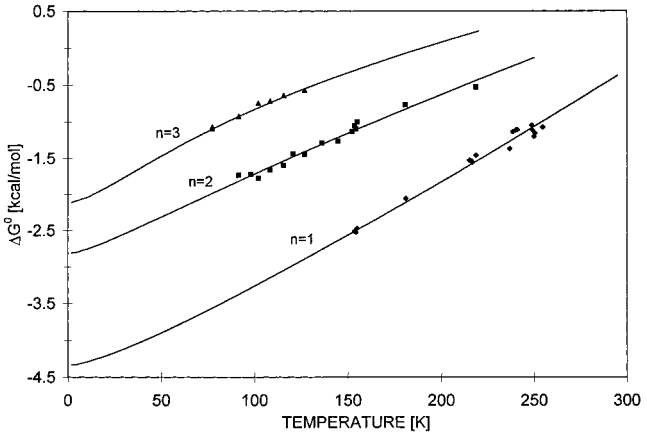

Figure 2. Plot of experimental ΔG_T° vs temperature for the association reaction $Cu^{+*}(H_2)_{n-1} + H_2 \rightarrow Cu^{+*}(H_2)_n$ for electronically excited Cu^+ ($4s^13d^9$). The solid lines are statistical mechanical fits to the data which yield values of ΔH_0° at $T = 0$ K (see text).

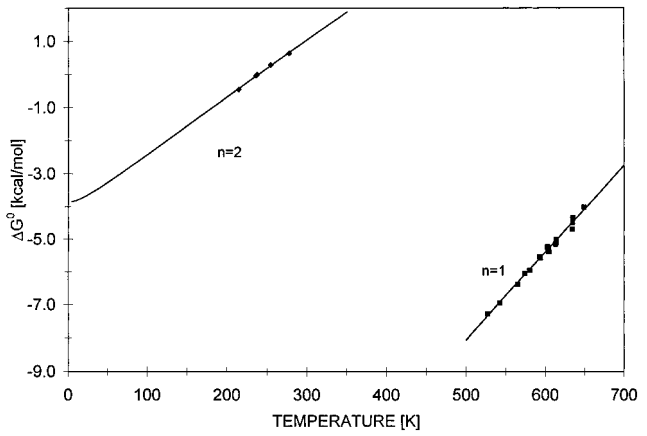

Figure 3. Plot of experimental ΔG_T° vs temperature for the association reactions of $H_2O{\cdot}Cu^+(H_2)_{n-1} + H_2 \rightarrow H_2O{\cdot}Cu^+(H_2)_n$. The solid lines are statistical mechanical fits to the data which yield values of ΔH_0° at $T = 0$ K (see text).

electronically excited clusters. For comparison, the ground-state clusters were also examined at the MP2 level.[24] The basis set used for the calculations is composed as follows. The hydrogen basis set is the scaled (4s)/[2s] set of Dunning,[25] augmented with a polarization p function ($\zeta p = 1.20$) and diffuse s ($\zeta s = 0.071$) and p functions ($\zeta p = 0.40$ and 0.13). The optimization of these exponents is described elsewhere.[18] The copper basis set is an [8s4p3d] contraction of the (14s9p5d) primitive set proposed by Wachters[26] supplemented with two diffuse p functions (we used the Wachter's exponents[26] multiplied by 1.5), one diffuse d function,[27] and a polarization f function.[28] This leads to a (14s11p6d3f)/[8s6p4d1f] contraction.[28] In most cases no significant differences in the DFT and MP2 geometries were found. The DFT bond strengths were generally higher, however. Care must be taken here since DFT calculations of the BDEs of the late metal ions with H_2 are unusually sensitive to the choice of basis set.[9,17a] Calculations by Maître and Bauschlicher have been previously reported on the $Cu^+(H_2)_{1,2}$ and the $H_2O{\cdot}Cu^+(H_2)$ ions.[18]

Results and Discussion

A summary of the experimental and theoretical enthalpies and experimental entropies for the ground- and excited-state association reactions is given in Table 1. Calculated vibrational frequencies are listed in Table 2. All of the cluster ions discussed here consist of an intact Cu^+ core ion surrounded by largely unperturbed H_2 ligands. No evidence of insertion was found.

Ground-State $Cu^+(H_2)_n$ Clusters. $Cu^+(H_2)$. The first H_2 ligand adds side on to the Cu^+ ion (in C_{2v} symmetry) and has a BDE of 15.4 kcal/mol. The cluster structure is nearly identical to that of other late metals such as $Co^+(H_2)$ and $Ni^+(H_2)$. The $Cu^+(H_2)$ BDE is similar to but about 15% smaller than that of $Co^+(H_2)$ and $Ni^+(H_2)$ (see Table 3 for a comparison). This is somewhat surprising since Cu^+ has a slightly smaller ionic radius than either Co^+ or Ni^+ [29] and we might expect that both the electrostatic and covalent attractions would be larger due to a closer approach. Theory indicates that bonding in all three ions is largely covalent and should be very similar. These covalent interactions consist mainly of donation from the H_2 σ orbital to the empty M^+ 4s orbital and back-donation from the filled $3d_{yz}$ ($d\pi$) orbital to the H_2 σ^* orbital. Both interactions cause an increase in the H−H bond length and a decrease in the H−H stretching frequency relative to the free H_2 (Figure 4 and Table 2). The origin of the lower bond strength in $Cu^+(H_2)$

(24) Frisch, M. J.; Trucks, G. W.; Schlegel, H. B.; Gill, P. M. W.; Johnson, B. G.; Wong, M. W.; Foresman, J. B.; Robb, M. A.; Head-Gordon, M.; Repogle, E. S.; Gomperts, R.; Andres, J. L.; Raghavachari, K.; Binkley, J. S.; Gonsalez, C.; Martin, R. L.; Fox, D. J.; Defrees, D. J.; Baker, J.; Stewart, J. J. P.; Pople, J. A. *Gaussian 92/DFT*, Revision G.2.; Gaussian, Inc.: Pittsburgh, PA, 1993.
(25) Dunning, T. H. *J. Chem. Phys.* **1970**, *53*, 2823.
(26) Wachters, A. J. H. *J. Chem. Phys.* **1970**, *52*, 1033.
(27) Hay, P. J. *J. Chem. Phys.* **1977**, *66*, 4377.
(28) Bauschlicher, C. W. *Theor. Chim. Acta* **1995**, *92*, 183.

Table 2. Theoretical Vibrational Frequencies for $Cu^+(H_2)_n$ Clusters[a,b]

ion	H−H stretch	asym. M^+-H_2 stretch	sym. M^+-H_2 stretch	$H_2-M^+-H_2$ bends and rotations
$Cu^+(H_2)$	3772	1146	881	
$Cu^+(H_2)_2$	3825, 3816	1202, 1202	934, 900	224, 224, 211
$Cu^+(H_2)_3$	3832(2), 3831	1128(2), 1116	817(2), 827	333 (2), 315, 273, 256 (2)
$Cu^+(H_2)_4$	3986(2), 3985, 3975	958, 954, 950(2)	722, 700(2), 659	280, 276, 259(2), 225, 93, 86, 59(2)
$Cu^{+*}(H_2)$	4089	534	454	
$Cu^{+*}(H_2)_2$	4115, 4093	476, 476	439, 313	267, 120, 46
$Cu^{+*}(H_2)_3$	4204, 4174, 4070	556, 487, 409	399, 311, 244	139, 110, 178
H_2	4422			

[a] Harmonic vibrational frequencies for the different $M^+(H_2)_n$ clusters as obtained by analytical differentiation of the SCF energy at the SCF geometry. The distinction between the different types of low-frequency modes is increasingly artificial for the larger clusters. [b] All numbers in cm^{-1}.

Table 3. $M^+(3d^n)$: Comparison of Binding Energies[a] for $M^+(H_2)_{n-1} + H_2 \rightarrow M^+(H_2)_n$

n	K^+	Ti^+	V^+	Cr^+	Fe^+	Co^+	Ni^+	Cu^+
1	1.45	10.0[b]	10.2	7.6	16.5[c]	18.2	17.3	15.4
2	1.35	9.7	10.7	9.0	15.7	17.0	17.6	16.7
3	−	9.3	8.8	4.7	7.5	9.6	11.3	8.8
4	−	8.5	9.0	3.4	8.6	9.6	7.1	5.1
5	−	8.2	4.2	1.4	2.2	4.3	4.2	1.0[f]
6	−	8.7	9.6[d]	1.1	2.3	4.0	0.8[f]	1.0
⟨BDE⟩[e]	1.4	9.1	8.6	4.5	8.8	10.5	11.5	11.5

[a] In units of kcal/mol. [b] Binding energy with respect to lowest d^3 configuration. [c] Binding energy with respect to lowest d^7 configuration. [d] The increase in $-\Delta H_0^\circ$ for $n = 6$ is due to a spin change from quintet to triplet on the core V^+ ion (see refs 5 and 18). [e] The sum of the binding energies divided by the total number of ligands (for the first solvation sphere). [f] Start of next solvation sphere.

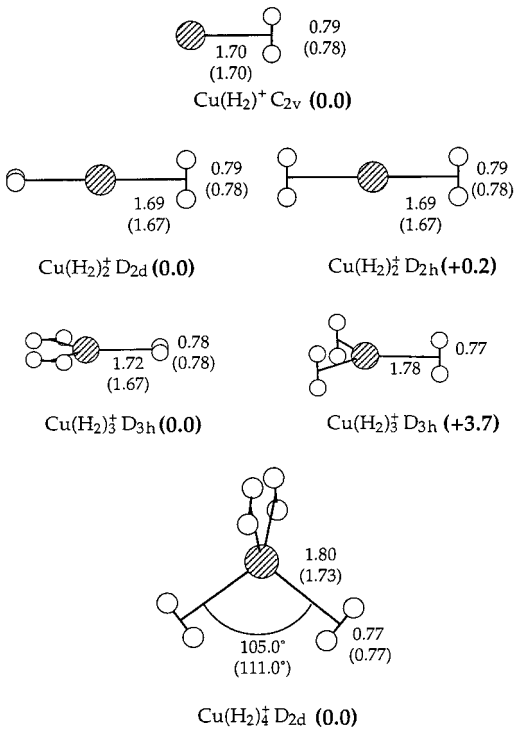

Figure 4. Theoretical geometries of the $Cu^+(H_2)_{1-4}$ ions calculated at the DFT B3LYP level (MP2 geometries are given in parentheses). All distances are in angstroms. Relative energies (in kcal/mol) for each isomer are given in parentheses.

is the filled $3d_{z^2}$ ($d\sigma$) orbital on Cu^+ which destabilizes the complex. In both $Co^+(H_2)$ and $Ni^+(H_2)$ the H_2 approaches a half-filled $3d_{z^2}$ orbital. The filled $3d_{z^2}$ orbital in Cu^+ both reduces σ donation from H_2 to Cu^+ and increases the on-axis repulsion between Cu^+ and H_2. Since most donation is into the empty Cu^+ 4s orbital, the decrease in donation is minor. The increase in repulsion is thus mainly responsible for the smaller BDE found for $Cu^+(H_2)$ relative to $Co^+(H_2)$ and $Ni^+(H_2)$. In $Co^+(H_2)$ and $Ni^+(H_2)$, where the $3d\sigma$ orbital is half-filled, calculations indicate $3d\sigma/4s$ hybridization reduces the M^+-H_2 repulsion by moving the *z* axis electron density to the *xy* plane.[9,13,17] This process requires a partial 3d−4s promotion, with the energy cost being recovered from the increased bond strength. In the case of the $Cu^+(H_2)$ ion, the filled $3d_{z^2}$ ($d\sigma$) orbital requires a promotion to a $4s^23d^8$ configuration to reduce the on-axis repulsion by an equivalent amount. This is a much higher energy process,[19] and the smaller $Cu^+(H_2)$ BDE reflects this. It seems clear, however, that this hybridization does occur to some extent in $Cu^+(H_2)$, since the second BDE is greater than the first (as in $Co^+(H_2)$ and $Ni^+(H_2)$, see Table 3).

Very similar arguments have been advanced to explain the bonding present in the $Cu^+(CO)_n$ ions.[11,30] The filled carbon σ orbital donates into the Cu^+ 4s orbital while the filled Cu^+ $d\pi$ orbitals ($3d_{xz}$ and $3d_{yz}$) donate into the CO $p\pi^*$ orbitals which are largely localized on the carbon. Hybridization of the Cu^+ 4s and $3d\sigma$ orbitals is used to reduce Pauli repulsion. Again, the σ and π dative interactions are synergistic: the π donation makes the CO more negative and thus better able to donate into the M^+ 4s orbital. The strength of the M^+-CO bond is much greater than that of M^+-H_2 (35.5[11] vs 15.4 kcal/mol). This is probably at least partly due to the use of the nonbonding CO σ orbital for donation (i.e., the CO bond is not weakened by the donation) and to the presence of two π interactions instead of one. Both $M^+(CO)$ and $M^+(H_2)$ show similar trends as the M^+ ion is changed. Both ligands have similar BDEs with Co^+,[8,10a] Ni^+,[9,10b] and Cu^+,[11] with the Cu^+ BDE about 10−15% smaller for both CO and H_2. The principal difference between the H_2 and CO ligands is that the M^+-H_2 bond strengths are about 40−45% of the M^+-CO values.

$Cu^+(H_2)_2$. The calculated structure of the $Cu^+(H_2)_2$ ion is shown in Figure 4. The second H_2 ligand binds opposite the first in D_{2d} symmetry with a measured BDE of 16.7 kcal/mol. This BDE is 1.3 kcal/mol larger than that of the first cluster. The similarity in the two bond strengths is also seen in the bond lengths and vibrational frequencies in the two clusters and is due to the similar interactions of the two H_2 ligands with Cu^+. In both cases, donation from the H_2 σ orbitals into the Cu^+ 4s orbital occurs as well as back-donation from the d_{yz} and d_{xz} ($d\pi$ orbitals) to the H_2 σ^* orbitals. The D_{2h} structure is 0.2 kcal/mol higher in energy than the D_{2d} because in D_{2h} symmetry back-donation to both ligands is from a single π-type orbital

(29) (a) Barnes, L. A.; Rosi, M.; Bauschlicher, C. W. *J. Chem. Phys.* **1990**, *93*, 609. (b) Desclaux, P. *Atomic Data Nucl. Data Tables* **1973**, *12*, 312.

(30) Barnes, L. A.; Rosi, M.; Bauschlicher, C. W. *J. Chem. Phys.* **1990**, *93*, 609.

(d_{yz}). A similar, small decrease in BDE with H_2 orientation is found in the $Co^+(H_2)_2$ case. Since the back-donation effect is estimated to add ~6 kcal/mol to the BDE,[18] this rather minor decrease in bond strength with axial H_2 rotation shows that a single dπ orbital can back-donate to two H_2 ligands almost as efficiently as two separate dπ orbitals. It also indicates that little, if any, polarization of the Cu^+ dπ orbital occurs (toward the H_2 σ^* orbital) since this would greatly favor the D_{2d} structure in the second cluster.

The linear ground-state structure found for $Cu^+(H_2)_2$ is similar to that of the other late metal complexes ($Fe^+(H_2)_2$, $Co^+(H_2)_2$, and $Ni^+(H_2)_2$). This is in contrast to the early metals where bent structures are either favored (as in $Sc^+(H_2)_2$[2] and $Ti^+(H_2)_2$)[3] or are low in energy ($V^+(H_2)_2$).[4] This preference for bent structures with the early metals is due to the presence of two empty 3d orbitals which can accept both in-phase and out-of phase electron donation from the H_2 σ orbitals (or in the case of the first excited state of $V^+(H_2)_2$ (which is bent), a single empty $3d_{xy}$ and an sd hybrid orbital). On-axis repulsion is not an issue since the 3dσ orbitals are empty. In the late metals, however, all of the 3d orbitals are at least half-filled. Because of this, donation into the 3dσ orbital is small and repulsion becomes the determining factor. Now the linear geometry is preferred because s/d hybridization efficiently minimizes the on axis repulsion of both ligands. The increase in BDE from the first to second cluster is due to this s/d hybridization. The symmetric hybridization increases the second ligand bond strength as well as the first, but the associated energy cost is paid in the first addition.[13]

Again the carbonyl system mimics the dihydride due to the similar bonding mechanisms present. The $Cu^+(CO)_2$ ion is linear with both CO ligands donating into the Cu^+ 4s orbital and both accepting electron density from the Cu^+ dπ orbital into their pπ^* orbitals.[31] The Cu^+ back-donating orbitals are thus shared by the two CO ligands, unlike the $Cu^+(H_2)_2$ case. The second CO BDE is about 15% greater than the first (35.5 vs 41 kcal/mol[11]), similar to the 8% increase seen with in the H_2 clusters. The larger increase in BDE in the carbonyl system is presumably due to the greater amount of sd hybridization present, relative to the dihydrogen system.

$Cu^+(H_2)_3$. The optimized DFT structure for the $Cu^+(H_2)_3$ ion is of D_{3h} symmetry with all atoms in the *xy* plane (see Figure 4). The BDE of the third H_2 ligand is much lower than that of the first two: 8.8 kcal/mol. This corresponds to an average BDE of 13.6 kcal/mol for three ligands vs 16.1 kcal/mol for the first two ligands. This decrease is not due to steric interference between the H_2 ligands. This can be shown theoretically by fixing the $H_2-Cu^+-H_2$ angle in $Cu^+(H_2)_2$ and then calculating the system energy *without* the Cu^+. As the angle is systematically decreased from 180° to 90°, no significant increase in energy results, showing the lack of H_2-H_2 interference (Figure 5). When the second cluster is constrained to a 120° $H_2-Cu^+-H_2$ bond angle (as in the third cluster) and the system is optimized with the Cu^+ ion present, a 3 kcal/mol per ligand destabilization is found relative to the 180° structure. This is similar to the experimental decrease in average BDE from the second to the third cluster and indicates that a reduction in the covalent interaction, rather than steric interference, is responsible for the decrease in BDE. In fact, the origin of both the highly symmetric structure and the marked decrease in bond strength lies primarily in the repulsive interaction of the H_2 σ orbitals with the filled 3d shell on Cu^+. In the planar D_{3h} structure, the three H_2 ligands have a repulsive σ interaction with three of the Cu^+ 3d orbitals (the $3d_{z^2}(a_1')$ and $3d_{x^2-y^2}/3d_{xy}(e')$, the *z* axis is the symmetry axis, see Figure 6a). The ion uses two methods to reduce this repulsion. First, the 4s and $3d_{z^2}$ orbitals are hybridized to move electron density from the *xy* plane to the $\pm z$ lobes. This hybridization is similar to that found in the first two clusters, but with an opposite shift in electron density. Second, and more important, the Cu^+ ion donates electron density from the repulsive $3d_{x^2-y^2}/3d_{xy}(e')$ pair of orbitals to the H_2 σ^* orbitals. This pair of orbitals is symmetry adapted to produce both two repulsive σ interactions *and* two attractive π interactions with the three ligands. The resulting π back-donation is similar in nature to that in the first two clusters, but in the third cluster, the back-donation also reduces the σ repulsion. This "push−pull" mechanism has the effect of increasing the extent of back-donation while (at the same time) reducing σ repulsion and is the primary driving force for the D_{3h} structure. Despite this, there is an overall reduction in back-donation in going from the second to the third cluster due to the greatly increased σ repulsion.

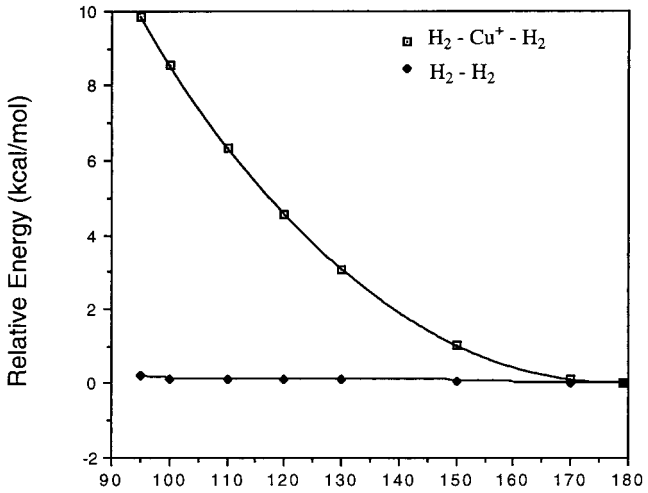

Figure 5. Relative energy of the $Cu^+(H_2)_2$ ion (calculated at the DFT level) as a function of the $H_2-Cu^+-H_2$ angle. All other geometrical parameters have been optimized for each fixed angle. The open squares correspond to the energy of the $Cu^+(H_2)_2$ ion, and the filled diamonds correspond to the energy of $(H_2)_2$ subsystem fixed at the optimized geometry of the $Cu^+(H_2)_2$. The lack of change in the $(H_2)_2$ system with changing angle shows that ligand−ligand repulsion is unimportant in this system. See text.

The remaining metal−ligand interactions are similar to those found in the first two clusters. Ligand to metal donation in $Cu^+(H_2)_3$ is again primarily from the H_2 σ orbital to the Cu^+ 4s orbital, although the natural bond order (NBO) population analysis indicates that a very small amount of $4p_{x,y}$ character may be present in the acceptor orbital (i.e., a minor amount of sp^2 hybridization). This would provide some directionality to the acceptor orbital for better overlap with the H_2 σ orbitals. The reduction in average BDE from 16.1 kcal/mol in the second cluster to 13.6 kcal/mol in the third is mainly a consequence of the increased σ repulsion (three ligands interacting repulsively with three orbitals vs two ligands interacting with one repulsive orbital). Although the repulsion is reduced through the mechanisms discussed, the result is a lower average bond strength. A very similar reduction in BDE is found between $Cu^+(CO)_2$ and $Cu^+(CO)_3$,[11] although no calculations have been done on the tricarbonyl system and no detailed understanding of the decrease has been presented.

The second (vertical) D_{3h} structure, with the H_2 ligands perpendicular to the *xy* plane, is 3.7 kcal/mol higher in energy and is actually a transition state (see Figure 4). The isomer spontaneously reverts to the planar form under an unconstrained

(31) Maître, P. Work in progress.

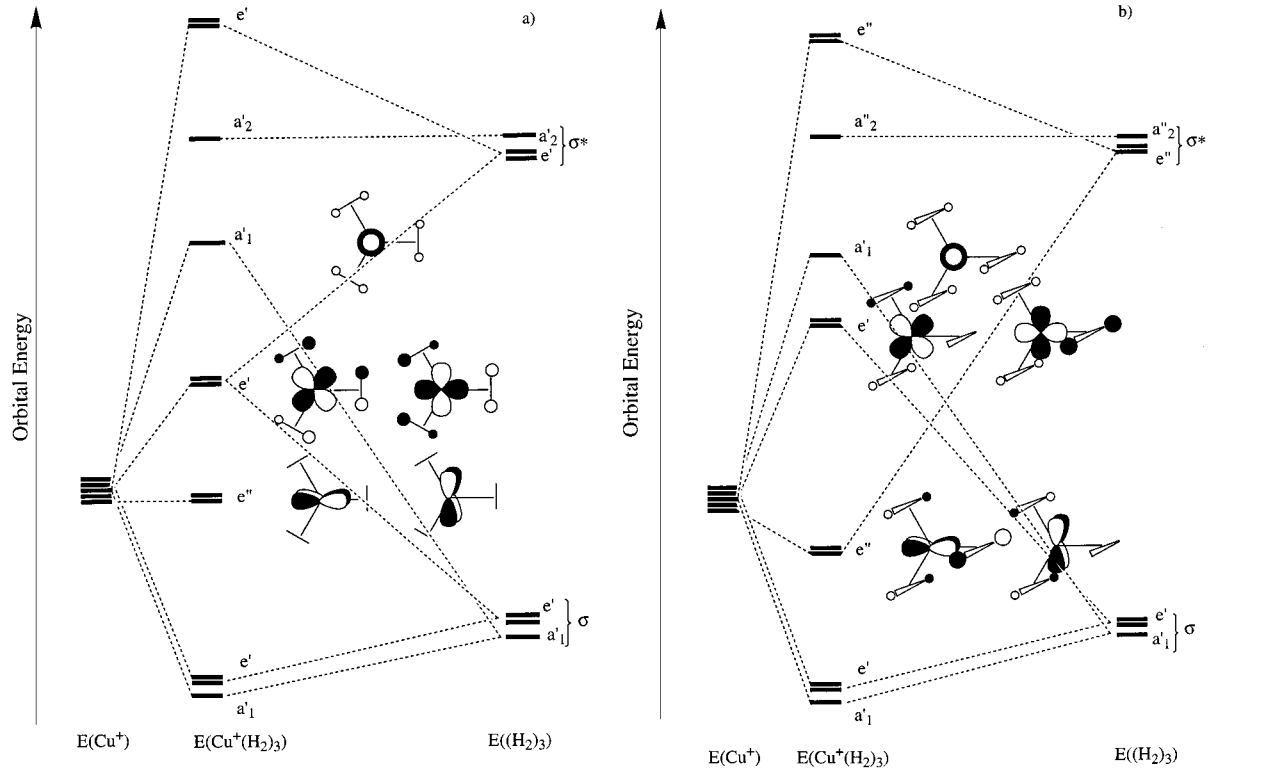

Figure 6. Relative energies of the molecular orbitals for the two lowest energy D_{3h} structures of $Cu^+(H_2)_3$: (a) planar geometry with all three H_2 molecular ligands lying in the *xy* plane (lowest energy structure); (b) vertical geometry with all three H_2 molecules perpendicular to the *xy* plane. In a, the lowest (a_1', e′) and highest (a_2', e′) pairs of orbitals are primarily symmetry-adapted sets of H_2 σ orbitals and σ^* orbitals while the center three MOs are primarily Cu^+ 3d orbitals. Similar assignments hold for the orbitals in b.

geometry optimization. This might seem surprising since the vertical and planar D_{3h} forms are superficially quite similar. They have nearly identical σ repulsion and the vertical isomer also has a degenerate pair of d orbitals available for back-bonding (the e″ set, $3d_{xz}/3d_{yz}$, see Figure 6b). Further, the vertical isomer has lower ligand−ligand repulsion (although this is a negligible effect). The destabilization of the vertical D_{3h} cluster is due to the loss of the very beneficial "push−pull" mechanism present in the planar geometry. In the vertical geometry, the back-donation from the e″ pair of orbitals does *not* lead to any reduction in σ repulsion. The result is a greatly reduced amount of back-donation, increased σ repulsion, and finally, a smaller bond energy. This can also be seen as a result of the splitting of the 3d orbital energies in the D_{3h} σ ligand field (the energy ordering is $3d_{z^2}(a_1') > 3d_{xy}/3d_{x^2-y^2}(e') > 3d_{xz}/3d_{yz}(e'')$) which reduces the 3d(e′)−H_2 σ^* energy difference and thereby enhances the π back-donation in the planar ion. Comparisons of the NBO populations, bond lengths and vibrational frequencies found in the two structures all show increased back-donation in the planar ion.

The preference for either the planar D_{3h} structure (as in $Cu^+(H_2)_3$ and $Ni^+(H_2)_3$) or a "T" geometry (as in $Co^+(H_2)_3$ and $Fe^+(H_2)_3$) is worth examining. As detailed above, steric effects can be discounted. Rather, the preference for the D_{3h} over a "T" structure depends on a symmetric population of the $3d_{xy}$ and $3d_{x^2-y^2}$ orbitals (the e′ set in D_{3h} symmetry). If these orbitals are both filled (as in $Cu^+(H_2)_3$ and $Ni^+(H_2)_3$), the D_{3h} geometry is favored for two reasons. First, the "push−pull" mechanism discussed above produces a large, synergistic back-donation which greatly enhances the bond strength and reduces σ repulsion. Second, the "T" structure is destabilized due to the extra metal−ligand repulsion in the *x*−*y* plane. If, on the other hand, one of these orbitals is only half-filled (as is required in $Fe^+(H_2)_3$ and $Co^+(H_2)_3$ to maintain a pure ground electronic configuration), the "push−pull" effect in the D_{3h} geometry is greatly reduced and the third H_2 will approach the $M^+(H_2)_2$ in a "T" configuration. In this geometry, all three H_2 ligands approach half-filled 3dσ orbitals which both minimizes repulsion and maximizes donation onto the metal ion. Further, if both the e′ and e″ orbital sets are half-filled (as in Cr^+), a D_{3h} geometry is also favored.[5] In this case, one-electron back-donation is used to reduce the σ repulsion, despite the fact that this is inherently less favorable than the two-electron process in $Cu^+(H_2)_3$.[13] Finally, the same conclusions about structural preference can be reached via a pure symmetry argument: the D_{3h} structure becomes unstable with respect to a Jahn−Teller distortion when the e′ and e″ sets of orbital are not equally occupied and a less symmetric "T" shape results.

In both $M^+(H_2)_3$ geometries, there is a reduction in BDE in going from the second to the third cluster. In ions which form a "T" structure ($Co^+(H_2)_3$[17] and $Fe^+(H_2)_3$[7,31]), this reduction in bond strength is mainly due to a reduction in the amount of s/d hybridization present in the second cluster as well as σ repulsion from a second 3d orbital. The s/d hybridization present in the second cluster produces a region of high electron density in the *xy* plane which the third H_2 must approach. As a result, the amount of s/d hybridization is reduced and the first two H_2 ligands are destabilized. (The electron cloud may also be partly polarized away from the third ligand using the 4p orbital as well,[7,17] but these orbitals are high in energy and the process is not as efficient as the s/d hybridization in the first two clusters.) As discussed above, the reduction in BDE in the clusters with the D_{3h} structure is due mainly to greater σ repulsion from the e′ and a_1' orbitals. To illustrate the importance of this repulsion in the D_{3h} geometry, note that the average BDE in the Ni^+ third cluster (with a half-filled $3d_{z^2}(a_1')$ orbital) is ∼2 kcal/mol greater than that in $Cu^+(H_2)_3$ (where the orbital is filled). In fact, $Ni^+(H_2)_3$, which has the optimum electron occupation for a D_{3h}

structure, has the highest average third BDE of all the transition metal ions (see Table 3).

$Cu^+(H_2)_4$. The $Cu^+(H_2)_4$ cluster closes the first solvation sphere. The ion is quasi-tetrahedral (D_{2d} symmetry, see Figure 4) with a BDE of 5.1 kcal/mol. This represents a 2.1 kcal/mol decrease in average BDE from the third cluster (from 13.6 to 11.5 kcal/mol), presumably due both to reduction in donation to Cu^+ from the H_2 ligands as well as increased σ repulsion. The BDE of $Cu^+(CO)_4$ is also much lower than $Cu^+(CO)_3$.[11] The effect of the $H_2-Cu^+-H_2$ bond angle is shown in Figure 5. When this angle is constrained to 105° (as in $Cu^+(H_2)_4$), there is a 1.3 kcal/mol reduction in average BDE relative to a 120° angle (as in $Cu^+(H_2)_3$). Thus the increased repulsion and decreased σ donation at the 105° angle accounts for a majority of the 2.1 kcal/mol decrease found experimentally. The amount of donation into the Cu^+ 4s orbital per H_2 ligand also becomes smaller in the larger clusters due to the greater number of ligands, further reducing the BDE. The reduction in σ donation in $Cu^+(H_2)_4$ is reflected in higher H−H stretching frequencies and shorter H−H bond lengths (more like free H_2). There is also a substantial increase in Cu^+-H_2 bond length (from 1.72 Å in the third cluster to 1.80 Å in the fourth, at the B3LYP level of theory). Back-donation in the third and fourth clusters is surprisingly similar. In $Cu^+(H_2)_4$, two of the three 3d orbitals which are symmetry adapted for back-donation are destabilized by σ repulsion, leading to the same "push−pull" effect found in $Cu^+(H_2)_3$.

Both $Cr^+(H_2)_4$ and $Ni^+(H_2)_4$ have similar D_{2d} quasi-tetrahedral structures. (The $Cu^+(CO)_4$ ion is highly symmetric with T_d symmetry.[31]) This may partly reflect the use of 4p acceptor orbitals (i.e., donation is partly into an sp^3 hybrid orbital on Cu^+), although the orbital population analysis is uncertain. Use of the 4p orbitals would allow both in-phase and out-of-phase contributions from the four H_2 ligands, which was an important stability factor in the $Ti^+(H_2)_n$ system.[3] Both $Fe^+(H_2)_4$[7] and $Co^+(H_2)_4$[17] also have distorted tetrahedral geometries, but here, the structure is derived from a "T"-shaped third cluster and the bonds are not all equivalent. Orbital populations do indicate that the 4p orbitals are partly responsible for these geometries as well, however.[17]

$Cu^+(H_2)_{5,6}$. Data for the $Cu^+(H_2)_5$ cluster could be obtained only at very low temperatures. Both the extremely weak BDE (1.0 kcal/mol) and, especially, the very small ΔS°_T show that this ligand is added in the second solvation shell. The very low vibrational frequencies, free H_2 rotations, and large rotational moments which result all give rise to more product entropy and make the ΔS°_T of association more positive (−12.5 cal/(mol·K) vs −20 to −24 cal/(mol·K) for the first four association reactions). Our DFT calculations are consistent with the observed increase in ΔS°_T. The lowest energy structure for $Cu^+(H_2)_5$ in the first solvation shell is a trigonal bipyramid (as in $Ni^+(H_2)_5$)); however, it is unbound with respect to the separated reactants ($Cu^+(H_2)_4 + H_2$, see Table 1). Data for the $Cu^+(H_2)_6$ cluster could be taken only at 77 K but matched that of the fifth cluster.

The $Co^+(H_2)_n$ and $Ni^+(H_2)_n$ systems have first solvation shells of six and five H_2 ligands, respectively.[8,9] This is due to the presence of two and one half-filled 3d orbitals (respectively). In $Co^+(H_2)_n$ the e_g ($3d_{x^2-y^2}/3d_{z^2}$) orbital set is half-filled and an octahedral arrangement results.[17] In $Ni^+(H_2)_5$ the single half-filled orbital leads to a stable trigonal bipyramid structure in which two polar H_2 ligands are attached to the D_{3h} core found in the third cluster.[9] Although this same D_{3h} structure is found in $Cu^+(H_2)_3$, the corresponding fifth cluster is not stable due to the filled $3d_{z^2}$ orbital which strongly destabilizes the two polar ligands. The result is a $Cu^+(H_2)_n$ solvation shell of four H_2 ligands. From a general chemistry viewpoint, the progressive reduction in the number of ligands in the first solvation shell illustrates the balance between the attractive forces in the complex and the occupation of the antibonding orbitals. The stability of $Co^+(H_2)_6$ shows that the destabilization resulting from single occupancy of the e_g orbitals is more than compensated for by the stabilization energy resulting from σ donation, π back-donation, and electrostatic attraction. It is not surprising, however, that adding one and two electrons to these antibonding orbitals results in the loss of one and two H_2 ligands from the hypothetical $Ni^+(H_2)_6$ and $Cu^+(H_2)_6$ octahedral clusters.

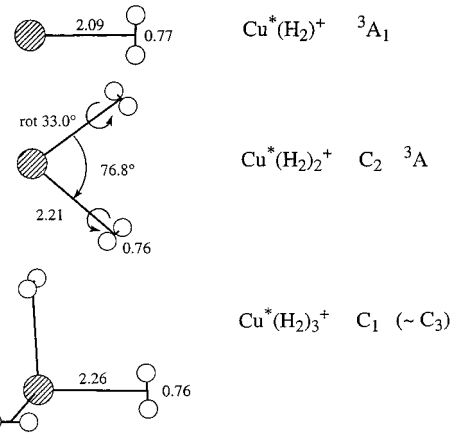

Figure 7. Theoretical geometries of electronically excited $Cu^+*(H_2)_{1-3}$ ions calculated at the DFT B3LYP level, assuming a ^3D, $4s^13d^9$ copper ion core configuration. All distances are in angstroms. Relative energies (in kcal/mol) for each isomer are given in parentheses.

Electronically Excited $Cu^+*(H_2)_n$ Clusters. Electronic state chromatography[21] showed that metastable excited copper ions are formed about a Cu^+ core with a $4s^13d^9$ valence configuration. Presumably this is the ^3D state (∼65 kcal/mol excitation[19]), but the ^1D state (75.1 kcal/mol[19]) may also be present since both states are metastable. In both excited states the large 4s orbital controls the interaction with H_2; hence, no significant difference between the bonding of these two states with H_2 is expected. Bond strengths are much weaker in these excited clusters, relative to the ground-state ions, due to the repulsive nature of the 4s electron.[13,32] The experimental ΔH°_T and ΔS°_T results are listed in Table 1, along with the derived BDEs and theoretical results for the triplet state. The calculated DFT structures for the triplet state clusters are shown in Figure 7.

Data were taken for the first three $Cu^+*(H_2)_n$ clusters. The BDEs are ∼20% of those found in the ground-state clusters (Table 1). There is a corresponding increase in Cu^+-H_2 bond length (from 1.70 to 2.09−2.26 Å, see Figures 4 and 7) and a decrease in the Cu^+-H_2 vibrational frequencies (Table 2). This is expected from the presence of the 4s electron which destabilizes the clusters in three ways: first, by greatly increasing the on-axis Pauli repulsion; second, by decreasing donation from the H_2 ligands to Cu^+ (normally into the 4s orbital); and third, by decreasing back-donation from the Cu^+ because of the much longer bond lengths.[13,32] These changes in the $Cu^+*(H_2)_n$ ions are also reflected in the more positive association entropies for the excited Cu^+* reactions (Table 1). The larger rotational moments and lower vibrational frequencies produce greater product entropy than the more tightly bound ground-state $Cu^+(H_2)_n$ ions.

(32) Armentrout, P. B. *Science* **1991**, *251*, 175.

Table 4. $M^+(4s^13d^{n-1})$: Comparison of Binding Energies[a] for $M^+(H_2)_{n-1} + H_2 \rightarrow M^+(H_2)_n$

n	Mn^+	Cu^+*	Zn^+
1	1.9	4.2	3.8
2	1.7	2.5	2.8
3	1.3	1.4	2.4

[a] In units of kcal/mol.

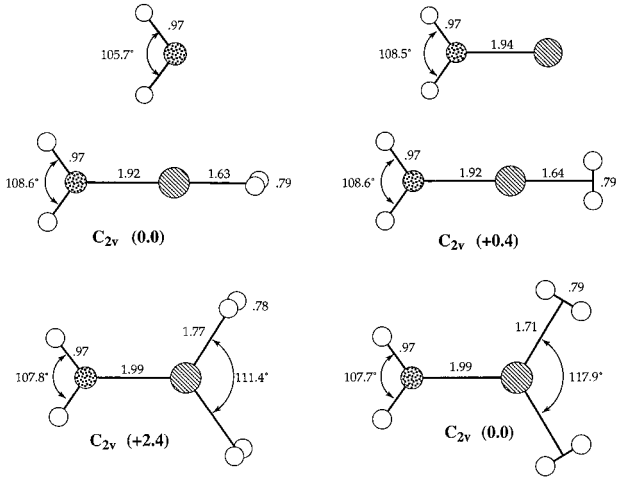

Figure 8. Theoretical geometries of the $H_2O{\cdot}Cu^+(H_2)_{1,2}$ ions calculated at the DFT B3LYP level. All distances are in angstroms. Relative energies (in kcal/mol) for each isomer are given in parentheses.

The Cu^+*$(H_2)_n$ ions can best be compared with the $Mn^+(H_2)_n$ and $Zn^+(H_2)_n$ systems which also have $4s^13d^{n-1}$ valence configurations with no low-energy $3d^n$ configurations available.[19] In all three cases, the H_2 ligands add at 90° to each other (i.e., along the *x*, *y*, and *z* axes).[6] This is due to the use of the 4p orbitals to polarize the 4s electron density away from the H_2 ligand. Three separate 4p orbitals are used for the first three ligands and bond angles of approximately 90° result. Table 4 shows that the Cu^+*$(H_2)_n$ and $Zn^+(H_2)_n$ systems have very similar BDEs while the $Mn^+(H_2)_n$ ions have a considerably lower bond strengths. The M^+-H_2 bond lengths are also similar in the Cu^+*$(H_2)_n$ and $Zn^+(H_2)_n$ systems and longer in the $Mn^+(H_2)_n$ ions. Both effects are consistent with the larger size of the 4s orbital in Mn^+.[29]

Finally we note that the Cu^+*(H_2) BDE appears to be somewhat greater than the corresponding $Zn^+(H_2)$ value (Table 4). This must be due to the presence of a half-filled $3d_{z^2}$ orbital in Cu^+*(H_2) which results in a smaller screening of the Cu^+ nuclear charge. We found that the lowest triplet state ($^3A_1'$) results from the Cu^+* electronic configuration in which the half-filled $3d_{z^2}$ orbital is oriented toward the H_2 ligands. The DFT calculations find that the $^3A_2$ state, where the $3d_{xy}$ is half-filled, has only about one-fourth of the ground-state binding energy and has a significantly longer Cu^+-H_2 bond length (2.28 vs 2.09 Å).

$H_2O{\cdot}Cu^+(H_2)_{1,2}$ Clusters. A summary of experimental and theoretical results for the $H_2O{\cdot}Cu^+(H_2)_{1,2}$ clusters is given in Table 5. Our calculated structures are shown in Figure 8, and the calculated vibrational frequencies are listed in Table 6. The $H_2O{\cdot}Cu^+(H_2)$ ion has been examined previously by Maître and Bauschlicher.[18] It is clear that addition of an H_2O ligand to Cu^+ has a rather dramatic effect on the subsequent H_2 binding energies. The experimental BDE of the second ligand increases from 16.7 to 19.6 kcal/mol when the first ligand is H_2O rather than H_2, while that of the third decreases from 8.8 to 3.8 kcal/mol. These changes in bond strength are also reflected in the Cu^+-H_2 bond lengths and frequencies. A similar increase in BDE for the addition of the first H_2 ligand was found both experimentally and theoretically in the $H_2O{\cdot}Co^+(H_2)$ ion.[8b,18]

In its lowest energy structure, $H_2O{\cdot}Cu^+(H_2)$ has C_{2v} symmetry with the H−H bond perpendicular to the H−O−H plane (Figure 8). The structure with the H−H bond coplanar is only 0.4 kcal/mol higher in energy and corresponds to a transition state in the rotation of the H_2 ligand about the Cu^+-H_2 bond. Bond lengths and cluster frequencies show little change between the two forms. Since this rotation should cause no change in σ repulsion, this result indicates that back-donation into the H_2 σ* orbital is only very slightly enhanced when the Cu^+ back-donating orbital ($3d_{yz}$) is destabilized by the oxygen lone pair (a π donor). It has been proposed that a significant amount of "pass through" back-donation might occur in this molecule, with the oxygen lone pair effectively donating to the H_2 ligand via the Cu^+ $3d\pi$ orbital,[33] thereby increasing the H_2 BDE in $H_2O{\cdot}Cu^+(H_2)$. Apparently, however, this is a minor effect, although it is probably the origin of the weak preference for the nonplanar C_{2v} ground-state structure. Instead, we think the origin of the increased BDE when water is attached lies in increased s/d hybridization. The Cu^+-H_2O bond is over twice as strong as the Cu^+-H_2 bond (37.6[34,35] vs 15.4 kcal/mol), and more s/d hybridization occurs (relative to the H_2 clusters) because there is a larger payback. This is shown experimentally by the large increase in BDE between the $Cu^+(H_2O)$ and $Cu^+(H_2O)_2$ ions (37.6 to 40.6 kcal/mol[34,35]) due to hybridization which has occurred in the first cluster. This increased s/d hybridization in $Cu^+(H_2O)$ increases the bond energy when an H_2 ligand is now added. As discussed above, this occurs in the pure M^+-H_2 cluster, but the increase in the second H_2 BDE is greater when the first ligand is H_2O because more hybridization has occurred with H_2O.

It is also interesting to look at the relative stabilities of the two-coordinate species and to observe that the reaction

$$Cu^+(H_2O)_2 + Cu^+(H_2)_2 \rightarrow 2H_2OCu^+(H_2) \qquad (3)$$

is about 4.1 kcal/mol exothermic. Not only does the H_2O ligand enhance the BDE of the subsequent H_2 ligand, but an H_2 first ligand similarly enhances the binding of a subsequent H_2O ligand. Such a thermodynamic effect has been observed in saturated species and is referred to as a "cis influence" or "static cis influence".[36]

This enhancement of the Cu^+-H_2 bond in $H_2O{\cdot}Cu^+(H_2)_n$ ends with the first H_2. The second H_2 is bound far more weakly than in the pure $Cu^+(H_2)_3$ clusters (3.8 vs 8.8 kcal/mol). This can be seen as a direct result of the enhancement of the first H_2 bond. The simultaneous s/d hybridization of the empty 4s acceptor orbital toward the H_2 and of the filled $3d_{z^2}$ away from the ligand yields a strong enhancement of the first H_2 ligand but is unfavorable to the approach of the second. The consequential reduction in hybridization directly reduces the second H_2 BDE. A similar loss occurs in the pure $Cu^+(H_2)_n$ clusters, but the enhancement of the first BDE is greater in the first $H_2O{\cdot}Cu^+(H_2)$ ion and consequently the reduction in BDE with the next addition is greater.

The structure of the $H_2O{\cdot}Cu^+(H_2)_2$ ion is planar with C_{2v} symmetry (Figure 8). This is analogous to the planar D_{3h}

(33) Perry, J. Private communication.
(34) Dalleska, N. F.; Honma, K.; Sunderlin, L. S.; Armentrout, P. B. *J. Am. Chem. Soc.* **1994**, *116*, 3519.
(35) Rosi, M.; Bauschlicher, C. W. *J. Chem. Phys.* **1990**, *92*, 1876.
(36) Cotton, F. A.; Wilkinson, G. *Advanced Inorganic Chemistry*, 5th ed.; J. Wiley and Sons: New York, 1988.

Table 5. Data Summary for $H_2O{\cdot}Cu^+(H_2)_n$ Clusters

	experimental				theoretical		
ion	BDE (D_0)[a]	$-\Delta H_T^\circ$ [a]	$-\Delta S_T^\circ$ [b]	T [c]	symmetry	D_e[a,d]	D_0[a,d]
$Cu\,H_2O^+$	37.6 ± 1.8[e]	−	−	−	C_{2v}	43.2	41.6 37.3[f]
$H_2O{\cdot}Cu^+(H_2)$	19.6 ± 0.9[g]	21.4 ± 0.8	26.6 ± 2	590 ± 60	C_{2v}[h]	22.2	18.8
					C_{2v}[i]	21.8	TS[j]
$H_2O{\cdot}Cu^+(H_2)_2$	3.8 ± 0.5[g]	4.1 ± 0.4	12.5 ± 2	245 ± 35	C_{2v}[i]	6.3	3.7
					C_{2v}[h]	3.9	TS[j]

[a] In kcal/mol. BDE $\equiv -\Delta H_0^\circ$. [b] In cal/(mol·K). [c] In Kelvin, ± refers to temperature range, not uncertainty. [d] DFT geometries and energies. [e] Reference 34. [f] Reference 35. [g] Fitting with theoretical frequencies and geometries. [h] Vertical C_{2v} structure (with H_2 ligand(s) rotated 90° with respect to the H−O−H plane). [i] Planar C_{2v} structure (all atoms in same plane). [j] Transition state.

Table 6. Theoretical Vibrational Frequencies for $H_2O{\cdot}Cu^+(H_2)_n$ Clusters[a,b]

ion	O−H stretch	H−O−H bend	Cu−OH_2 modes	H−H stretch	asym. Cu−H_2 stretch	sym. Cu−H_2 stretch	H_2−CuH_2O bends and torsions
CuH_2O^+	3780, 3873	1646	431,610,155				
$H_2O{\cdot}Cu^+(H_2)$	3780, 3871	1648	466, 619, 186	3703	1330	933	214, 214, 265
$H_2O{\cdot}Cu^+(H_2)_2$	3803, 3884	1659	395, 580, 124	3793, 3800	1142, 1137	837, 795	326, 333, 258, 147, 223, 246

[a] Harmonic vibrational frequencies for the different $M^+(H_2)_n$ clusters as obtained by analytical differentiation of the SCF energy at the SCF geometry. The distinction between the different types of low-frequency modes is increasingly artificial for the larger clusters. [b] All numbers in cm^{-1}.

structure found with $Cu^+(H_2)_3$ and a similar "push−pull" effect where σ repulsion drives the π donation operates here as well. A second C_{2v} structure exists for the $H_2O{\cdot}Cu^+(H_2)_2$ ion with the H_2 ligands parallel with the oxygen lone pairs (Figure 8). This is analogous to the vertical D_{3h} isomer of $Cu^+(H_2)_3$. As in $Cu^+(H_2)_3$, however, the planar orientation of the H_2 is significantly more stable. This shows again that the in-plane 3d orbitals, destabilized by the σ orbitals of the ligands, are best suited for back-donation.

Conclusions

(1) Bond dissociation energies and association entropies were determined for $Cu^+(H_2)_{1-6}$, indicating that the first four H_2 ligands form the first solvation shell while the fifth and sixth H_2 ligands begin the second solvation shell.

(2) Molecular geometries and vibrational frequencies were determined from extensive calculation at the DFT and MP2 levels.

(3) Bonding in the clusters consists mainly of donation to Cu^+ from the H_2 σ orbital, back-donation from the Cu^+ 3dπ orbitals to the H_2 σ^* orbital, and the charge-induced dipole and charge quadrupole electrostatic attractions. These interactions in $Cu^+(H_2)_n$ are similar to those found in $Co^+(H_2)_n$ and $Ni^+(H_2)_n$ but slightly weaker due to the increase in Pauli repulsion caused by the filled 3d shell in $Cu^+(H_2)_n$.

(4) Electronically excited $Cu^{+*}(H_2)_{1-3}$ clusters (with a Cu^+, $4s^13d^9$ configuration) were also examined and found to have much weaker bond energies, similar to $Zn^+(H_2)_n$ and $Mn^+(H_2)_n$. The large repulsive 4s orbital was responsible.

(5) Addition of an H_2O ligand increased the bond strength of the first H_2 ligand but dramatically reduced the BDE for the second H_2. These effects were explained in terms of increased s/d hybridization between the Cu^+ and H_2O relative to the pure H_2 clusters.

(6) Remarkably similar trends were found in the $Cu^+(H_2)_n$ and in the $Cu^+(CO)_n$ systems with the Cu^+-H_2 BDEs ~45% of the Cu^+-CO values. This is due to the very similar M^+-ligand interactions in both systems. This same correspondence is also present in the corresponding Ni^+ and Co^+ systems.

Acknowledgment. The support of the National Science Foundation under Grant CHE-9729146 is gratefully acknowledged. P.W. thanks the "Deutscher Akademischer Austauschdienst" for financial support. P.M. thanks the scientific committee of IDRIS for a generous allocation of computer resources (Project 96079).

JA9822658